

# Time-dependent dielectric breakdown measurements of porous organosilicate glass using mercury and solid metal probes

Dongfei Pei and Michael T. Nichols

*Plasma Processing and Technology Laboratory, Department of Electrical and Computer Engineering, University of Wisconsin-Madison, Madison, Wisconsin 53706*

Sean W. King and James S. Clarke

*Intel Corporation, Hillsboro, Oregon 97124*

Yoshio Nishi

*Department of Electrical Engineering, Stanford University, Stanford, California 94305*

J. Leon Shohet<sup>a)</sup>

*Plasma Processing and Technology Laboratory, Department of Electrical and Computer Engineering, University of Wisconsin-Madison, Madison, Wisconsin 53706*

(Received 6 June 2014; accepted 15 July 2014; published 4 August 2014)

Time-dependent dielectric breakdown (TDDB) is one of the major concerns for low-k dielectric materials. During plasma processing, low-k dielectrics are subjected to vacuum ultraviolet photon radiation and charged-particle bombardment. To examine the change of TDDB properties, time-to-breakdown measurements are made to porous SiCOH before and after plasma exposure. Significant discrepancies between mercury and solid-metal probes are observed and have been shown to be attributed to mercury diffusion into the dielectric porosities. © 2014 American Vacuum Society.

[<http://dx.doi.org/10.1116/1.4891563>]

## I. INTRODUCTION AND BACKGROUND

Interconnection RC delay time is one of the major problems in back-end-of-line (BEOL) components for integrated circuits.<sup>1</sup> The RC delay can be reduced by either lowering the resistance of the conductors or the capacitance between the conductors. To reduce the capacitance, materials with low dielectric constant are used in BEOL integration. The low-k porous organosilicate glass (OSG or SiCOH)<sup>2,3</sup> is widely used as a low-k material to replace the role of SiO<sub>2</sub> as the intermetal dielectrics. One of the most critical challenges for SiCOH in this application is the time dependent dielectric breakdown (TDDB).<sup>4</sup> TDDB is the process of breakdown after the dielectric material is held under a relatively low electric field stress for a long time. The TDDB lifetime of the dielectric can be influenced by several factors, including electric stress, temperature, contacting metals (capping layers), plasma processing, and curing processing.<sup>5</sup> The TDDB lifetime of most dielectric materials is in the scale of years under the normal operating electric fields. To study the TDDB property of low-k materials over a short time period, higher temperature and higher electric stress are applied to these dielectrics so as to accelerate the breakdown.<sup>6</sup>

During plasma processing, vacuum ultraviolet (VUV) radiation and ion bombardment take place and create both defect states and trapped charge inside low-k dielectric materials.<sup>7,8</sup> These exposures can affect the dielectric constant,<sup>9</sup> breakdown voltage,<sup>10</sup> leakage current,<sup>11</sup> and hydrophilicity.<sup>12</sup> The TDDB properties will also change after plasma processing.<sup>13</sup>

TDDB measurements of dielectric materials have been made under constant voltage, constant time, ramping voltage, and ramping current.<sup>4</sup> Both the time-to-failure (TTF) and charge-to-failure (CTF) can be measured to represent

the TDDB properties. Previous work on porous SiCOH using mercury probe as the measurement tool has shown that the plasma processing will downgrade both TTF and CTF. In addition, using the mercury probe, the CTF versus electric field curve shows a significant peak after plasma exposure.<sup>13</sup> That is, the measurements showed that the CTF was lower at lower electric fields as well as at higher electric fields. The lower charge at lower electric fields is counterintuitive.

## II. EXPERIMENTAL MEASUREMENTS

In order to resolve this issue, TDDB of porous SiCOH was measured before and after plasma exposure using both the mercury probe and a solid metal pin probe with deposited titanium metal contacts. This comparison was done because TDDB is not only a dielectric property; it is also affected by the contacting metal. In this case, the comparison is between mercury and titanium contacts. A hexagonal pattern of titanium was deposited on a porous SiCOH film grown on a silicon substrate. The area of each hexagon is  $2.8 \times 10^{-4}$  cm<sup>2</sup> and the layer thickness is 200 nm. A constant voltage is applied over the porous SiCOH film, and the leakage currents are measured as a function of time. At the breakdown point, the amplitude of the leakage current increases by more than four orders of magnitude. The time to reach the breakdown point is recorded as the TTF. The CTF can be found by integrating the leakage current over time until breakdown. Each measurement was repeated several times under the same condition and Weibull statistics<sup>14</sup> were used to analyze the TDDB data and find the characteristic lifetime and total charge to breakdown.

The porous dielectric SiCOH measured in this paper was deposited on a Si wafer using plasma-enhanced chemical vapor deposition. After deposition, the film was UV cured

<sup>a)</sup>Electronic mail: shohet@engr.wisc.edu

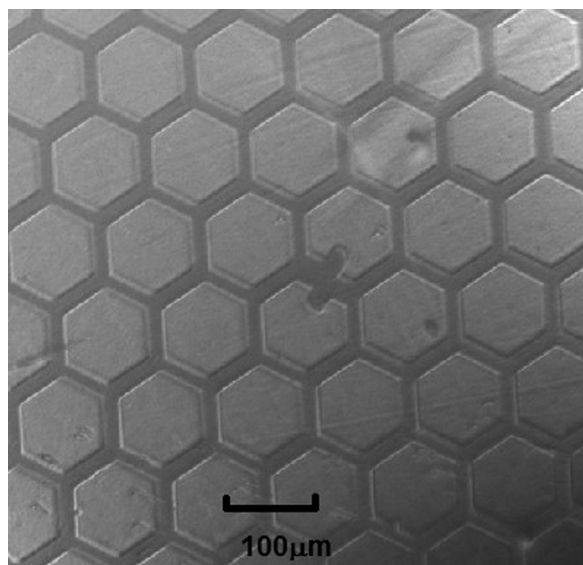


Fig. 1. Hexagonal array pattern of titanium deposited on the porous low- $k$  SiCOH sample. The distance between adjacent hexagons is  $20\ \mu\text{m}$  and the thickness of the metal is  $200\ \text{nm}$ .

with an ultraviolet thermal processing system. The photons used in this curing process had the energy between  $3.1$  and  $6.2\ \text{eV}$ , and the photon fluence was approximately  $10^{16}$  photons/cm<sup>2</sup>. The thickness of the porous SiCOH film was  $500\ \text{nm}$  after UV curing, and the relative dielectric constant was  $2.55$ . The density of the film was  $1.24\ \text{g/cm}^3$ , and the porosity was measured to be  $15\%$ – $20\%$ .

An electron-cyclotron-resonance argon plasma was used to process the material. The selected plasma condition generated VUV radiation peaked at  $11.6$  and  $11.8\ \text{eV}$  as well as ion bombardment with energy around  $100\ \text{eV}$ . The time of plasma exposure was controlled so that the photon fluence was approximately  $10^{16}$  photons/cm<sup>2</sup> and the ion fluence was  $10^{17}\ \text{cm}^{-2}$ .

As mentioned above, there are two methods to make contact with the sample. The first one uses a mapping mercury probe (MDC 862). The contact area of the mercury and sample was  $4.5 \times 10^{-3}\ \text{cm}^2$ . The other method uses a probe station. As described above, a hexagonal array pattern of titanium was deposited on the porous SiCOH samples before and after plasma exposure using thermal evaporation. The hexagonal structure size was  $7 \times 10^{-5}\ \text{cm}^2$  on a side and had a thickness of  $200\ \text{nm}$ , as shown in Fig. 1. The pin probe station was then used to make contact with the hexagon to apply the constant voltage. A program-controlled picoammeter with an internal DC power supply was used to apply a constant voltage to the porous SiCOH film and measure the leakage currents. Both the mercury and the pin probes were positively biased, and the silicon substrate was grounded. A controlled heater was used to change the temperature when the sample was placed under pin probe. The heating temperature was  $110^\circ\text{C}$ . Based on previous work,<sup>15</sup> no significant effects of water desorption at this temperature were seen. No heating was done for the mercury-probe measurements. The range of bias voltages was chosen so that the electric field over the porous SiCOH film was between  $1.5$  and  $7.5\ \text{MV/cm}$ .

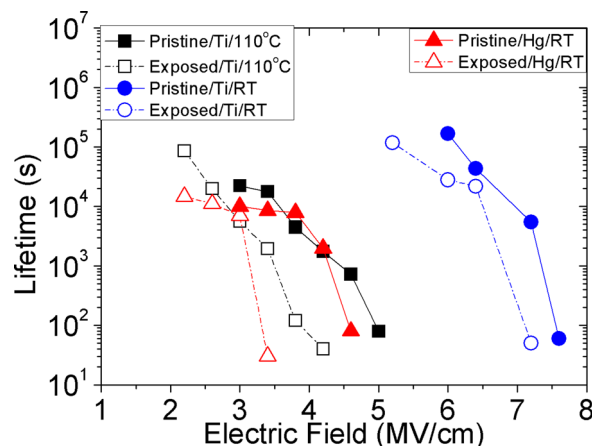


Fig. 2. (Color online) Lifetime (66.2% TTF) of porous SiCOH as a function of electric field under different conditions. Pin probe on titanium (Ti): Pristine (without plasma exposure) and plasma-exposed samples at room temperature (RT) and  $110^\circ\text{C}$ . Mercury probe (Hg): Pristine and plasma-exposed sample at room temperature.

Figure 2 shows the characteristic lifetime of porous SiCOH as a function of electric stress for the pristine and plasma-exposed samples. There is a clear degradation of the TDDDB properties of the porous SiCOH film after plasma exposure. This trend can be seen in both the pin probe and mercury probe measurements under different temperatures. This agrees with previous work.<sup>13</sup> Figure 2 also shows a difference in the time-to-failure versus electric field between the two different measuring systems. The breakdown lifetime of porous SiCOH measured with the mercury probe changes slowly over a range of relatively low electric field (less than  $4\ \text{MV/cm}$  for the pristine sample and less than  $3.2\ \text{MV/cm}$  for the plasma-exposed sample) and then drops rapidly to a low value after a certain point. However, using the titanium contact and probe station, there was no sudden decrease in the TTF as the electric field increases. Thus, the difference between the two contacting methods indicates that the metal contact is likely to have played an important role in the dielectric breakdown.

Figure 3 shows the charge-to-breakdown of porous SiCOH versus electric stress for the pristine and plasma-exposed

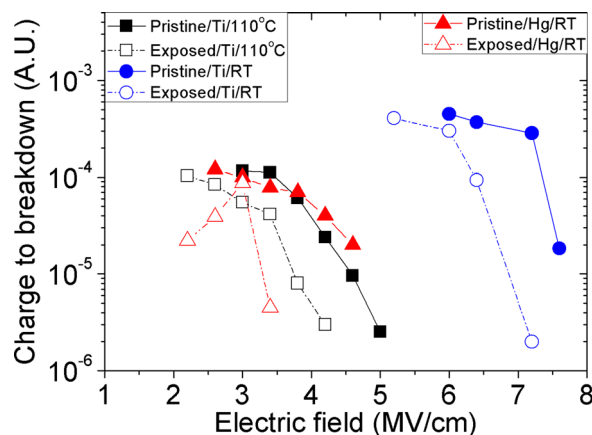


Fig. 3. (Color online) Charge-to-breakdown of porous SiCOH as a function of electric field under different conditions. Pin probe on titanium (Ti): Pristine and plasma-exposed samples at RT and  $110^\circ\text{C}$ . Mercury probe (Hg): Pristine and plasma-exposed samples at room temperature.

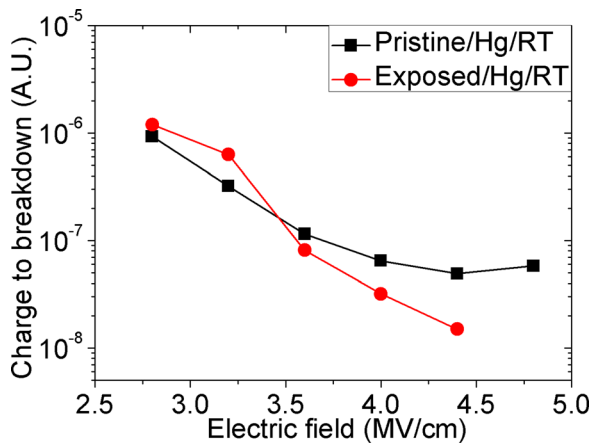


Fig. 4. (Color online) Charge-to-breakdown of nonporous SiCOH as a function of electric field at RT using the mercury probe (Hg). Pristine and plasma-exposed samples are compared.

samples. Both the pin- and mercury-probe measurements show a degradation of the TDDB properties of the porous SiCOH after plasma exposure as the charge-to-breakdown gets smaller after the plasma exposure. However, the measurements show a significant difference depending on the nature of the metal contact. The measurements using the pin probe with the titanium contact shows that charge-to-breakdown decreases as the electric field increases. However in the case of the mercury-probe measurements, the charge-to-breakdown first increases as the electric field increases at low field and then decreases after about 3 MV/cm, resulting in an unexpected peak on the curve as shown in Fig. 2. This effect only occurs for the plasma-exposed sample using the mercury probe. This indicates the likelihood of an additional failure mechanism caused by the presence of the mercury contact.

### III. DISCUSSION AND CONCLUSIONS

Previous work has shown that plasma exposure can change the surface properties of porous SiCOH including its pore structure and hydrophilicity.<sup>12,15</sup> Thus, a likely explanation of the “peak” effect is from the diffusion of mercury into the dielectric film. Compared with titanium, mercury is more likely to diffuse into the porous SiCOH dielectric, but this diffusion effect is not very strong for pristine UV-cured films. However, after plasma exposure, additional defect states and/or open pores on or near the surface of the porous SiCOH film can appear. This will enhance the mercury diffusion and will hasten the breakdown process. As a result, less charge is needed for the dielectric to break down. This effect is more significant at low electric fields because the breakdown time is longer and thus more time is available for mercury to diffuse into the dielectric film. The peak in Fig. 2 was not seen in the case of the titanium contact.

To further investigate this assumption, the same measurements were made on a nonporous SiCOH film. The measurement results using the pin probe and the mercury probe are shown in Fig. 4. It is seen that the CTF curves do not seem to vary significantly from each other. This is as expected.

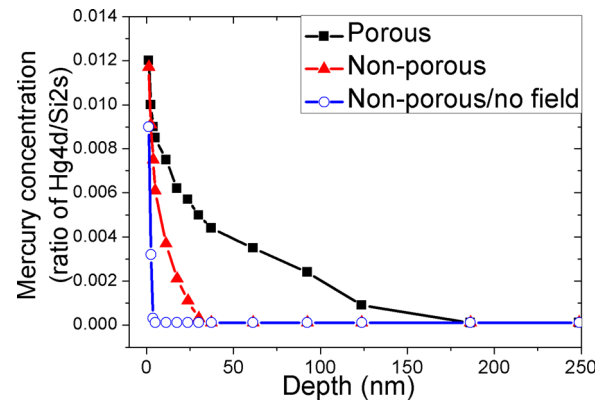


Fig. 5. (Color online) Density vs depth profile of mercury in samples after TDDB measurement with mercury probe with and without the electric field. The samples include: (1) plasma-exposed porous samples after TDDB measurement with mercury probe with electric field (rectangles), (2) plasma-exposed nonporous samples after TDDB measurement with mercury probe with electric field (triangles), and (3) plasma exposed nonporous samples after 30 h of contact with mercury probe (circles), but no electric field.

In order to measure the mercury diffusion or migration into the plasma-exposed samples, x-ray photoelectron spectroscopy (XPS) measurements were made. Four different kinds of samples were measured with the mercury probe. The first two samples were porous and nonporous SiCOH held under 3 MV/cm until breakdown occurred. The other two samples were the same porous and nonporous SiCOH in contact with the mercury for 30 h (longer than the breakdown time under 3 MV/cm) but no electric field was applied. Then XPS was used to analyze the mercury concentrations within the films. An ion gun was used to etch the films to obtain a depth profile of the mercury concentration. Figure 5 shows the measured results. The ratio of the amplitude of the mercury peak (Hg4d) to the silicon peak (Si2s) amplitude was calculated to represent the relative concentration of mercury at different depths of the sample. Without the electric field, no mercury was detected inside the low-k film. With the electric field present, mercury was detected in both the porous and nonporous SiCOH. However, the mercury penetration depth of the porous sample is around 100 nm deeper than the depth for the nonporous sample (about 20 nm). Considering that the typical interlayer dielectric thickness is less than 100 nm, the penetration depth of mercury is very large even for the nonporous sample.

We conclude that it is much easier for mercury to migrate into porous SiCOH films under an electric field. There are two possible reasons. (1) Some mercury ions are formed under the electric field and then drift into the SiCOH film. (2) The electric field applied to the porous SiCOH creates a pressure that forces mercury atoms to electromigrate into the film. The existence of mercury inside the film will shorten the effective thickness of the dielectric film, making it easier to break down under the same voltage.

To summarize, both mercury probe and pin-probe measurements show a degradation of the TDDB properties of porous SiCOH after plasma exposure. However, the measurements with the mercury probe showed a peak on the

charge-to-breakdown versus electric field for plasma-exposed porous SiCOH, but the pin-probe data does not show this peak. This effect is believed to occur because mercury migration into the porous SiCOH is significantly enhanced in porous SiCOH. Because of this effect, the use of mercury probes on porous SiCOH has to be done with caution.

## ACKNOWLEDGMENTS

This work was supported by the Semiconductor Research Corporation under Contract No. 2012-KJ-2359 and by the National Science Foundation under Grant No. CBET-1066231.

<sup>1</sup>H. B. Bakoglu and J. D. Meindl, *IEEE Trans. Electron. Devices* **32**, 903 (1985).

<sup>2</sup>A. Grill, *J. Appl. Phys.* **93**, 1785 (2003).

<sup>3</sup>K. Maex, M. R. Baklanov, D. Shamiryan, F. Iacopi, S. H. Brongersma, and Z. S. Yanovitskaya, *J. Appl. Phys.* **93**, 8793 (2003).

<sup>4</sup>E. Anolick and G. Nelson, *Proceedings of the International Reliability Physics Symposium* (1979), pp. 8–12.

<sup>5</sup>C. Guedj, E. Martinez, and G. Imbert, *Materials Research Society Symposium Proceedings* (2007), p. 990.

<sup>6</sup>R. Chang, Y. Yue, and S. Wong, *Dig. Tech. Pap. - Symp. VLSI Technol.* **2002**, 18.

<sup>7</sup>C. Cismaru and J. L. Shohet, *Appl. Phys. Lett.* **74**, 2599 (1999).

<sup>8</sup>S. Uchida, S. Takashima, M. Hori, M. Fukasawa, K. Ohshima, K. Nagahata, and T. Tatsumi, *J. Appl. Phys.* **103**, 073303 (2008).

<sup>9</sup>J. M. Atkin, E. Cartier, T. M. Shaw, R. B. Laibowitz, and T. F. Heinz, *Appl. Phys. Lett.* **93**, 122902 (2008).

<sup>10</sup>J. R. Lloyd, E. Liniger, and T. M. Shaw, *J. Appl. Phys.* **98**, 084109 (2005).

<sup>11</sup>J. M. Atkin, D. Song, T. M. Shaw, E. Cartier, R. B. Laibowitz, and T. F. Heinz, *J. Appl. Phys.* **103**, 094104 (2008).

<sup>12</sup>D. Shamiryan, M. R. Baklanov, S. Vanhaelemeersch, and K. Maex, *J. Vac. Sci. Technol., B* **20**, 1923 (2002).

<sup>13</sup>M. T. Nichols, H. Sinha, C. A. Wiltbank, G. A. Antonelli, Y. Nishi, and J. L. Shohet, *Appl. Phys. Lett.* **100**, 112905 (2012).

<sup>14</sup>E. Y. Wu, E. J. Nowak, R. P. Vollertsen, and L. K. Han, *IEEE Trans. Electron. Devices* **47**, 2301 (2000).

<sup>15</sup>X. Guo, J. E. Jakes, M. T. Nichols, S. Banna, Y. Nishi, and J. L. Shohet, *J. Appl. Phys.* **114**, 084103 (2013).